PHYSICAL REVIEW B **85**, 155448 (2012)

Influence of surface passivation on the friction and wear behavior of ultrananocrystalline diamond and tetrahedral amorphous carbon thin films

A. R. Konicek,[1,*] D. S. Grierson,[2] A. V. Sumant,[3] T. A. Friedmann,[4] J. P. Sullivan,[4] P. U. P. A. Gilbert,[5] W. G. Sawyer,[6] and R. W. Carpick[7]

[1]*Physics & Astronomy Department, University of Pennsylvania, Philadelphia, Pennsylvania 19104, USA*
[2]*Mechanical Engineering Department, University of Wisconsin-Madison, Madison, Wisconsin 53706, USA*
[3]*Center for Nanoscale Materials, Argonne National Laboratory, Argonne, Illinois 60439, USA*
[4]*Sandia National Laboratory, Albuquerque, New Mexico 87185, USA*
[5]*Physics Department, University of Wisconsin-Madison, Madison, Wisconsin 53706, USA*
[6]*Mechanical and Aerospace Engineering Department, University of Florida, Gainesville, Florida 32611, USA*
[7]*Mechanical Engineering and Applied Mechanics, University of Pennsylvania, Philadelphia, Pennsylvania 19104, USA*

(Received 1 February 2012; published 25 April 2012)

Highly sp^3-bonded, nearly hydrogen-free carbon-based materials can exhibit extremely low friction and wear in the absence of any liquid lubricant, but this physical behavior is limited by the vapor environment. The effect of water vapor on friction and wear is examined as a function of applied normal force for two such materials in thin film form: one that is fully amorphous in structure (tetrahedral amorphous carbon, or ta-C) and one that is polycrystalline with <10 nm grains [ultrananocrystalline diamond (UNCD)]. Tribologically induced changes in the chemistry and carbon bond hybridization at the surface are correlated with the effect of the sliding environment and loading conditions through *ex situ*, spatially resolved near-edge x-ray absorption fine structure (NEXAFS) spectroscopy. At sufficiently high relative humidity (RH) levels and/or sufficiently low loads, both films quickly achieve a low steady-state friction coefficient and subsequently exhibit low wear. For both films, the number of cycles necessary to reach the steady-state is progressively reduced for increasing RH levels. Worn regions formed at lower RH and higher loads have a higher concentration of chemisorbed oxygen than those formed at higher RH, with the oxygen singly bonded as hydroxyl groups (C-OH). While some carbon rehybridization from sp^3 to disordered sp^2 bonding is observed, no crystalline graphite formation is observed for either film. Rather, the primary solid-lubrication mechanism is the passivation of dangling bonds by OH and H from the dissociation of vapor-phase H_2O. This vapor-phase lubrication mechanism is highly effective, producing friction coefficients as low as 0.078 for ta-C and 0.008 for UNCD, and wear rates requiring thousands of sliding passes to produce a few nanometers of wear.

DOI: 10.1103/PhysRevB.85.155448 PACS number(s): 81.05.ug, 62.20.Qp, 68.37.Xy, 61.05.cj

I. INTRODUCTION

Smooth, ultrahard, nearly hydrogen-free (H-free), highly pure carbon films have exceptional tribological properties—namely, low friction and wear without any liquid lubricant—but their widespread application is limited by the dependence of this physical behavior on the vapor environment. Along with their exceptional mechanical and chemical properties, in certain environments, particularly those possessing passivating vapor species like water and molecular hydrogen, these films exhibit extremely low friction coefficients and wear rates for long periods of time, even under highly loaded conditions. This paper focuses on the environmental dependence of the tribological properties of two of these materials, tetrahedral amorphous carbon (ta-C) and ultrananocrystalline diamond (UNCD), since they are among the most promising nearly H-free carbon films proposed as solid lubricants. The UNCD films in this study have a typical as-grown surface roughness of ∼11 nm r.m.s. over a 1×1 μm^2 area, 2–5 nm grains, and exhibit 95–98% sp^3 bonding overall.[1] The ta-C films have an as-grown surface roughness of ∼0.1 nm r.m.s. over a 1×1 μm^2 area and are comprised of an amorphous network of carbon that is ∼80% sp^3-bonded, with the remaining ∼20% being sp^2 bonded.[2] These are two of the smoothest carbon films of their respective types. Since they are both predominantly comprised of sp^3-bonded carbon, they have a modulus and hardness[3–5] that approach the values for single-crystal diamond.[6] These materials are being used in applications encompassing a wide range of length scales, from the nanoscale as atomic force microscope probes,[7,8] to the microscale as structural materials for microelectromechanical systems,[5,9,10] to the macroscale as coatings on mechanical seals for automotive engine components.[11] While researchers have investigated the environmental dependence of their tribological properties as self-mated solid lubricants to some degree,[11–13] further work is needed to completely understand the tribological properties and wear mechanisms of these films as solid lubricants.

Overall, there has been less work published on the tribological behavior of ta-C compared to polycrystalline diamond films [e.g., micro- or nanocrystalline diamond (MCD or NCD)] and other amorphous carbon films (both hydrogenated and nonhydrogenated), and few experiments have investigated the tribological properties of ta-C as a self-mated solid lubricant. For both UNCD and ta-C, the work performed[12–20] consistently shows that tribochemical reactions—surface chemical modifications induced by sliding contact—have a strong influence on wear. This is true not only for the flat surface of a tribological test, but also for the counterface.[21] Hydrogen or hydroxyl groups, produced from the dissociation of water (liquid or vapor), alcohols (liquid), or H_2 (vapor), have

been shown to chemically passivate surface carbon dangling bonds that are created during sliding. This is hypothesized to reduce friction and wear by preventing carbon-carbon bonding across the sliding interface. For example, in an environment containing water or hydrogen, self-mated friction coefficients can be as low as ∼0.07 for ta-C,[22] and ∼0.005 for UNCD,[19] while in inert atmospheres (e.g., highly pure nitrogen or argon gas) or vacuum, the friction coefficients for both materials increase by one to two orders of magnitude.[13,19,22] Matta *et al.* performed self-mated pin-on-disk studies with H-free amorphous carbon (a-C) and ta-C coated on ruby and sapphire substrates in an H_2 environment.[12] The ta-C film in their study was grown by cathodic arc deposition, had a Young's modulus of ∼650 GPa, and is mentioned to have more sp^3-bonded carbon than the a-C films grown by sputter-ion deposition (Young's modulus ∼250 GPa). After over one meter of sliding in 10 Torr partial pressure of H_2, the a-C achieved a low friction coefficient, and TOF-SIMS revealed that the surface was hydrogenated. The ta-C film showed similar performance. Prioli *et al.* examined the effect that relative humidity (RH) has on ta-C friction and found that there was no significant change in ta-C friction between 5.0–80.0% RH.[23] They suggested that this is due to the hydrophobic nature of amorphous carbon. Matta *et al.* tested the effect of lubrication on the friction behavior of amorphous carbon films grown by various methods that have a high sp^3-bonding percentage (∼90%).[16] They saw that the lubricant hydroxylated the ta-C, creating an OH-terminated surface, which reduced interactions across the interface and lowered friction. Similarly, self-mated ta-C films exhibit friction coefficients below 0.01 in glycerol, but friction coefficients approached 1 in ultrahigh vacuum (UHV).[20] In the same report, time-of-flight secondary ion mass spectroscopy (TOF-SIMS) from a sample tested with deuterated glycerol detected fragments of H, ^{2}H, OH, and O^{2}H at higher concentrations from regions inside the wear track than outside. This is consistent with the hypothesis that hydrogenation and hydroxylation passivate the surfaces to reduce friction and wear. Others have shown with Raman and TOF-SIMS that for a self-mated hydrogenated DLC interface, both the wear track and the debris undergo significant oxidation when worn in air.[24] However, these methods neither identify the exact types of oxygen bonding (single or double bonding), nor their relative concentrations produced by tribological sliding.

Molecular dynamics (MD) has been used to examine the effect that material properties (such as composition and structure) and surface properties (such as the presence or absence of hydrogen) have on the mechanical and tribological performance of H-free amorphous carbon[25–28] and diamond[25,29] at the nanoscale. Gao *et al.* used a reactive empirical bond-order (REBO) potential, which had been modified to better reproduce the mechanical properties of graphite and diamond, to study how the sp^3/sp^2 fraction of H-free amorphous carbon films will change the tribological behavior.[25] MD simulations were carried out using H-terminated single crystal diamond sliding against either single crystal diamond substrates or amorphous carbon films (of different thicknesses) on top of diamond substrates. This was the first work to show that, for diamond-like carbon, removing hydrogen from one counterface (in this case diamond) increased the sliding friction between the two surfaces. They also concluded that surfaces with a higher fraction of sp^2-bonded carbon are likely to exhibit higher friction. The sp^2-bonded carbon atoms in the film undergo tribochemical reactions whereby they formed chemical bonds across the interface, leading to atomic-scale wear events. Such processes would presumably produce wear in a macroscopic experiment and thereafter change the contact pressure and adhesion at the interface. They also examined a diamond-diamond interface and found that, for loads less than ∼130 nN, diamond had lower friction than the amorphous carbon films, but at higher loads the friction increased nonlinearly and became much higher compared to the H-free amorphous carbon.

Researchers have also examined the effects that surface roughness and film composition have on the friction behavior of polycrystalline diamond films. Erdemir *et al.* compared the friction behavior between rough and smooth (350 and 30 nm r.m.s., respectively) polycrystalline diamond counterfaces in ambient air and found that the number of run-in cycles was higher for the rougher counterface.[30] Hayward *et al.* tested polycrystalline diamond samples before and after a mechanical polishing treatment and found that the rougher sample (210 nm r.m.s.) required ∼30 run-in cycles before reaching steady-state, whereas the polished sample (35 nm r.m.s.) had almost no evidence of run-in, with each sample having a similar steady-state friction coefficient of ∼0.16 with linear reciprocation under a 2.0 N load and at 0.3 mm^1s^{-1}.[31] They concluded that run-in depends on surface roughness, and that the friction will decrease only after the interface has been smoothed by abrasive wear. These results confirm that rough diamond films are highly abrasive and exhibit higher friction initially, with friction reducing only as the diamond roughness is reduced by tribological sliding. Chromik *et al.* studied the effect that the film growth conditions had on the run-in behavior of polycrystalline diamond films being worn by a sapphire pin with linear reciprocation under a 6.4 N load and at 1 mm^1s^{-1}.[15] During growth, the hydrogen flow rate was varied between 0–36% of the total flow, yielding films with varied roughness, sp^2 fraction, and grain size. Their results were in partial disagreement with the Hayward work: the rougher the film, the fewer the number of cycles required to run in to steady-state friction. One reason for the differences between these two studies may arise from the fact that the films studied by Hayward *et al.* were grown by different methods, so, in addition to the surface roughness, the bulk and surface composition were likely different for the samples tested. In particular, in Chromik *et al.*, the rougher films had more sp^2-bonded carbon. As well, the polishing used in Hayward *et al.* likely modified the chemical nature of the surface significantly. Furthermore, different pin types and geometries were used as the counterfaces during testing, which would alter the loading conditions (e.g., contact pressure) and affect the run-in and steady-state friction behavior. Therefore the effect that roughness, surface chemistry, and loading might have on run-in can not be fully separated. The results of Chromik *et al.* highlight the fact that, although the surface roughness is an important factor when considering the run-in behavior, the chemical structure of the film (namely, the sp^2 bonding fraction) also plays a critical role in determining how

the contact evolves during run-in. Diamond can either be an abrasive or a low-friction material depending on the roughness and the surface chemistry.

Run-in is an extremely important characteristic since many applications cannot provide the necessary energy it takes to undergo run-in and are intolerant of the debris that forms during the run-in period, until the system reaches a steady state. However, a carefully measured and systematic study of the effect of environment on the number of run-in cycles has not been reported for H-free carbon films. Here, for the first time, we examine the run-in and steady-state behavior of UNCD and ta-C by varying the normal load and relative humidity to gain insight into the mechanisms that govern friction and wear for these tribologically exceptional materials. With respect to ta-C, this is the first systematic investigation into its tribological properties as a function of environment and normal load for self-mated interfaces with spectroscopic characterization of the modified surfaces. In contrast with our experimental approach, the aforementioned studies compared films where the bulk and surface properties were modified before examining the friction run-in behavior.

II. EXPERIMENT

Si flats (1×1 cm^2) and Si_3N_4 spheres (Cerbec, 3 mm diameter, grade 3) were simultaneously coated with either ta-C or UNCD. The ta-C films were deposited at Sandia National Laboratory using a pulsed laser deposition technique with a thickness of $\sim$1 μm.[9] A graphite target was ablated as the carbon source. As-grown ta-C films have a relatively high amount of residual compressive stress ($\sim$8 GPa), and so a post-growth annealing at 600 °C for 5 minutes was applied to all ta-C films to relieve the stress.[32] The annealing causes a restructuring of the film that relieves stress without significantly changing the bonding hybridization.[33]

UNCD was deposited at Argonne National Laboratory using a 2.45 GHz microwave plasma chemical vapor deposition technique (iPlas, 49.2/0.8 Ar/CH_4 gas chemistry, 140 mbar, 780 °C).[34] These films were 1–2 μm thick. Near-edge x-ray absorption fine structure (NEXAFS)[34] and Raman[35] spectra on the flats produced the signatures unique to high-quality UNCD.

After deposition on the flats and spheres, these films were subjected to self-mated reciprocating tribometry tests using a tribometer (described more fully here[36]) housed inside an environmentally controlled chamber. Normal and lateral forces were measured with a calibrated dual-flexure cantilever. In all cases, the number of sliding cycles (5000) was chosen to ensure steady-state friction behavior (i.e., stable friction not changing appreciably over time). The reciprocation length was set to 600 μm for every track, with a reciprocation rate of 2.5 Hz. Friction coefficient measurements were obtained from data averaged over the middle 90% of the track, where the velocity was nominally constant, thus ignoring the turnabout regions of the track where the sample was accelerating or decelerating. Humidity was introduced by controlling the flow of dry argon through a beaker containing deionized water. Relative humidity was measured with a DewPro MMY 2650 hygrometer, which is accurate within $\pm$0.1%, with a lower detection limit of 0.1%.

Two studies were considered for each type of film. For the first study, henceforth referred to as the constant-load study, the applied load was fixed (1.0 N for UNCD, corresponding to an initial mean Hertzian contact pressure of 649 MPa, and 0.5 N for ta-C, corresponding to an initial mean Hertzian contact pressure of 517 MPa), and four different values of relative humidity (RH) were used (1.0%, 2.5%, 5.0%, and 50.0%). For the second study, henceforth referred to as the load/RH study, a load ten times lower, i.e., 0.1 N for UNCD (initial mean Hertzian contact pressure of 300 MPa) and 0.05 N for ta-C (initial mean Hertzian contact pressure of 240 MPa), was used at both 1.0% and 50% RH. Including the 1.0% and 50% RH tracks at the higher loads, a set of four tracks is considered for this load/RH study: low load/low RH, low load/high RH, high load/low RH, high load/high RH. Thus a total of six tracks were made per sample: four tracks at a fixed load (specific to each film) at different RH levels and two tracks at the highest and lowest RH levels, but with one tenth the respective applied load. Each track was made using an unworn sphere; thus six different spheres were used to create the six tracks on each sample. The test conditions are listed in Table I. Note that the constant-load study (four tracks per sample) and the load/RH study (four tracks per sample) involve analyzing two of the same tracks per sample (at 1% and at 50% RH for the higher load used for each sample). Thus these data sets are repeated in comparison plots of each study.

Wear volumes and wear rates of the spheres and flats were determined from profilometry measurements (Zygo NewView 6300). All measurements were taken at a higher magnification than previously published results, using improved image analysis techniques to achieve more accurate topographies.[13] Since the wear volume measurements are taken just once at the end of the tribometer test, they are referred to as "single-point" values. As far more wear occurs initially, single-point measurements do not provide steady-state wear rate information, but instead provide an upper-bound value. Track widths are defined as the distance across the middle of the track between the points that intersect the plane of the surrounding surface. The wear volume of the flat is calculated by summing the depths all pixels inside the track that are below the plane of the surrounding surface, and multiplying those depths by the area of a pixel. For a wear track that is 600 μm long and 50 μm wide, and assuming the uncertainty in the height of every pixel is 1 nm, there would be an uncertainty in the measured wear volume of 2.9×10^{-8} mm^3. Considering a track with a low measured wear volume (ta-C with a 0.05 N load, 50.0% RH) for 5000 cycles and a 600 μm track length, this would be a wear rate uncertainty of 9.8×10^{-8} mm^{3}N^{-1}m^{-1}. We used the calibrated profilometry data to ascertain the worn area of the sphere. The wear volume was subsequently calculated by geometric considerations using the worn area dimensions and the sphere radius.

The wear tracks were analyzed *ex situ* using photoelectron emission microscopy (PEEM) on beamline 7.3.1.1 at the Advanced Light Source. PEEM is a surface-sensitive technique that characterizes the top $\sim$4 nm of the sample with $\sim$50 nm lateral resolution.[37] The chemical information comes from the near-edge x-ray absorption fine structure (NEXAFS) spectra acquired in conjunction with the spatial information of PEEM. The benefit PEEM-NEXAFS yields for tribochemistry studies,

TABLE I. Compiled tribometry and wear data for both materials. All wear rate values are single-point wear rate calculations.

Material	μ_{ss}	Number of run-in cycles	Track with (μm)	Average track depth	Track with rate	Sphere wear rate
ta-C						
0.5 N, 1.0%RH	0.59	N/A	155	299 nm	2.4×10^{-5} mm^3/Nm	5.5×10^{-6} mm^3/Nm
0.5 N, 2.5%RH	0.075	920	90	16 nm	9.7×10^{-7} mm^3/Nm	7.3×10^{-7} mm^3/Nm
0.5 N, 5.0%RH	0.078	340	57	8 nm	2.3×10^{-7} mm^3/Nm	1.3×10^{-7} mm^3/Nm
0.5 N, 50.0%RH	0.046	3	44	5 nm	8.5×10^{-8} mm^3/Nm	5.1×10^{-8} mm^3/Nm
0.05 N, 1.0%RH	0.163	9	21	5 nm	5.0×10^{-7} mm^3/Nm	1.5×10^{-8} mm^3/Nm
0.05 N, 50.0%RH	0.139	5	35	4 nm	5.2×10^{-7} mm^3/Nm	2.1×10^{-7} mm^3/Nm
UNCD						
1.0 N, 1.0%RH	0.015	2000	177	1495 nm	$\ll 3.8 \times 10^{-5}$ mm^3/Nm	1.7×10^{-5} mm^3/Nm
1.0 N, 2.5%RH	0.018	660	169	721 nm	1.6×10^{-5} mm^3/Nm	9.7×10^{-8} mm^3/Nm
1.0 N, 5.0%RH	0.008	49	41	10 nm	9.1×10^{-8} mm^3/Nm	5.5×10^{-8} mm^3/Nm
1.0 N, 50.0%RH	0.021	3	14	7 nm	7.8×10^{-8} mm^3/Nm	2.6×10^{-8} mm^3/Nm
0.1 N, 1.0%RH	0.028	600	27	5 nm	1.2×10^{-7} mm^3/Nm	3.9×10^{-8} mm^3/Nm
0.1 N, 50.0%RH	0.029	350	18	4 nm	1.2×10^{-7} mm^3/Nm	5.0×10^{-8} mm^3/Nm

beyond high spatial and energy resolution, is its ability to simultaneously image both worn and unworn portions of the sample. The images and spectra acquired predominantly came from the center of each track. Due to the acceleration and deceleration at the ends of each track, the center is where the exposure time (i.e., the time between passes over a given point) and friction are best controlled and measured. The edges of the track were also investigated to characterize the debris.

Since the PEEM analysis is performed *ex situ*, there can be chemical modifications to the track that occur after the tribotesting is finished. Samples are stored in clean dry nitrogen until they are examined in the PEEM to prevent large amounts of contamination, but certainly the PEEM analysis does not correspond to the instantaneous surface chemistry present during sliding. Rather, since UNCD is hydrogen-terminated as grown, the samples are initially nearly free of oxygen with a known sp^2/sp^3 content. Increases in surface-bound oxygen or changes to the sp^2/sp^3 content, revealed by *differences* between worn and unworn regions in the PEEM, show whether tribochemical changes occur and are then interpreted in terms of the exposure conditions during tribometry.

III. RESULTS

The friction data from the constant-load study for ta-C are plotted in Fig. 1(a), and key results for this and all other tests are listed in Table I. The test performed at 1.0% RH exhibits a high, fluctuating friction coefficient (~0.6) for all 5000 cycles. All other data have an interval of higher friction (run-in period) before eventually achieving a steady-state friction coefficient of ~0.04. Figure 1(b) highlights the difference in the run-in behavior of the track created at 50.0% RH compared to the others. Run-in for the 50.0% RH track occurs in 3 cycles, while the run-in requires 340 cycles for 5% RH, and 920 cycles for 2.5% RH. In other words, for each test that achieved low friction there is an inverse relationship between RH level and number of run-in cycles, and the steady-state friction coefficients slowly increase for higher sliding cycles. Note that an anomalously low friction coefficient is seen in the first 1–3 cycles for the high-friction tracks. This transient effect is likely due to sticking of the slider during the first few small-amplitude cycles.

The friction data from the constant-load UNCD tests are displayed in Fig. 2, with a magnified view of the first 100 cycles from Fig. 2(a) shown in Fig. 2(b). All UNCD friction coefficients eventually run in to approximately the same low-friction value of ~0.02. Similar to the ta-C results shown in Fig. 1(a), there exists a clear inverse relationship between

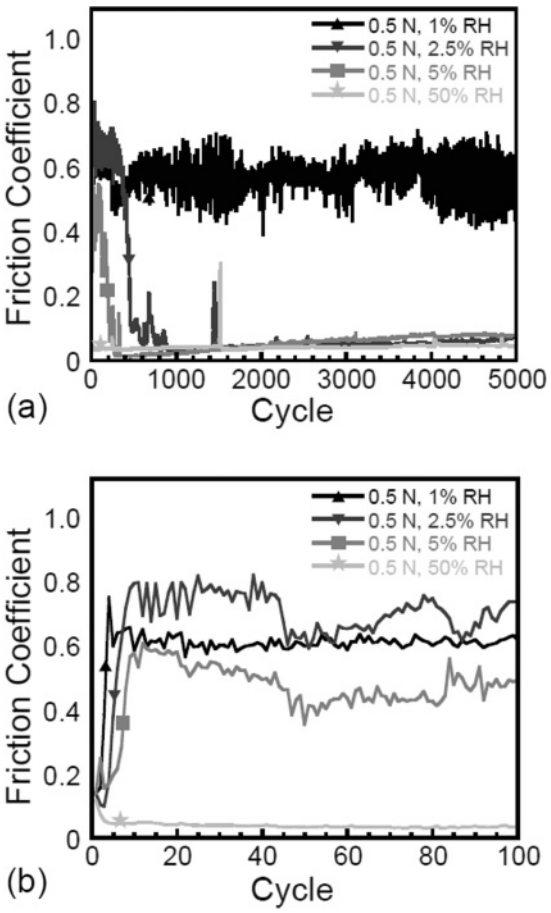

FIG. 1. (a) Friction plot for self-mated ta-C constant load study (0.5 N). (b) Zoom of first 100 cycles to highlight low-friction behavior for 50.0% RH track. All tracks were run for 5000 total cycles.

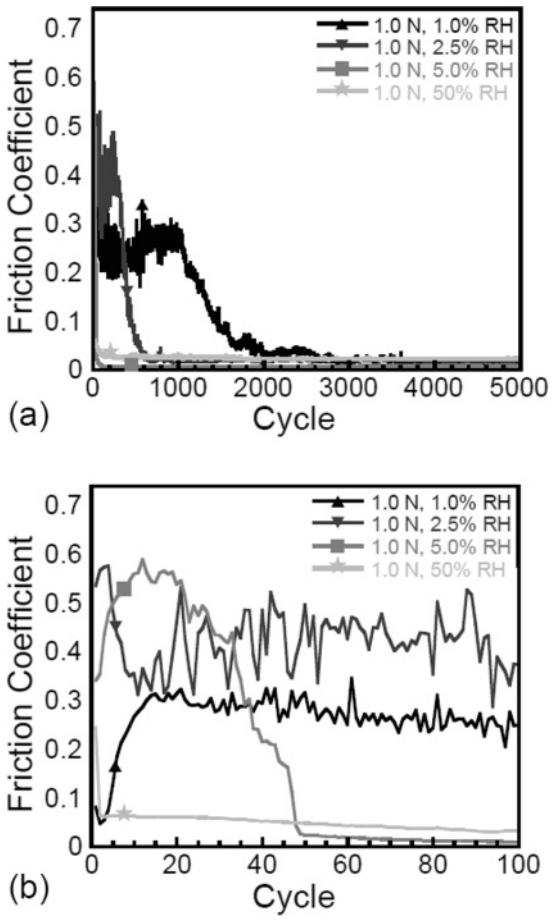

FIG. 2. (a) Friction plot for self-mated UNCD constant-load study (1.0 N). (b) Zoom of first 100 cycles to highlight low-friction behavior for 5.0% and 50.0% RH tracks. All tracks were run for 5000 total cycles.

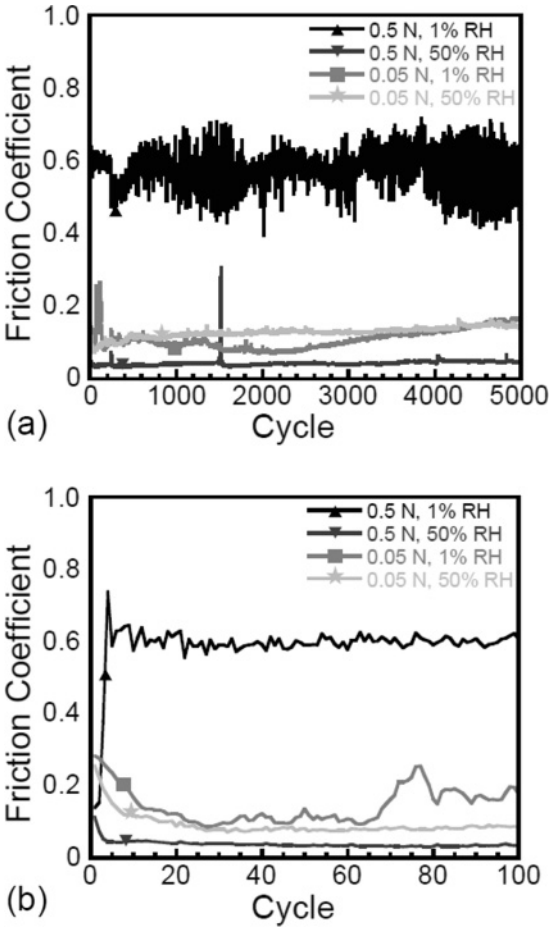

FIG. 3. (a) Friction plot for self-mated ta-C RH/load study. (b) Zoom of first 100 cycles to highlight high-friction behavior for the 1.0% RH track. All tracks were run for 5000 total cycles.

RH level and number of run-in cycles for UNCD. In contrast to ta-C, the UNCD friction coefficients do not increase with increasing sliding cycles after run-in.

The ta-C friction data from the load/RH study are shown in Fig. 3(a), and the first 100 cycles in Fig. 3(b). As already seen in Fig. 1(a), the track created at 0.5 N, 1.0% RH never achieves low friction. However, at the same humidity, with the load reduced to 0.05 N, the track runs in after ∼9 cycles, reaching a minimum friction value of 0.163. Also, as seen in Fig. 1(a), there is a transition in behavior as a function of RH between the two 0.5 N load tracks. The 0.5 N track created at 50.0% RH does run in quickly (within 3 cycles) and maintains low friction, unlike the 0.5 N track created at 1.0% RH, which showed sticking initially and then high friction subsequently. The ta-C load/RH study also reveals quantitative differences in the final friction values for the three tracks that ran in. The friction coefficient after run-in for the 0.5 N load test was 0.046 [see Fig. 3(a)]. This is less than one-third the value of the final friction coefficients for the 0.05 N tracks, made at 1.0% and 50.0% RH, which were 0.163 and 0.139, respectively.

Figures 4(a) and 4(b) show the equivalent load/RH study data for UNCD (detailed elsewhere[13]). For these UNCD tests, the tribometry results show that all four tracks (at high and low load, high and low humidity) ran in to a low friction value. The data followed the same trend seen for ta-C: tracks created at lower humidity and higher load experienced higher friction and higher wear. Similar to ta-C, the tracks made at higher load ran in to lower friction values (0.015 and 0.021) compared to the tracks made at the lower load (0.028 and 0.029).

The profilometry results (see Table I) provide the wear track dimensions from the flats and spheres, and were used to calculate wear rates. For all the studies on both ta-C and UNCD there are clear correlations between the load and RH level during the test and the number of run-in cycles, track width, average track depth, track wear rate, and sphere wear rate. The tracks created with higher loads and lower humidities had shorter sliding lengths (only ∼420–560 μm) compared to the tracks created at lower loads, since the higher static friction prevented longer sliding distances. It is unclear from the profilometry if this evolved with the number of sliding cycles. Tracks that had high friction over a longer number of cycles had deeper and wider wear tracks, and therefore higher wear rates. This reduced the average contact pressure at the interface. These also corresponded to higher sphere wear. For example, for ta-C, the track created at 0.5 N, 50.0% RH ran in within 3 cycles, had a final width of only 44 μm, and had a single-point wear rate of 8.5×10^{-8} mm^{3}N^{-1}m^{-1}. In contrast, the 0.5 N, 2.5% RH track took 920 cycles to run in, had a final width of 90 μm, and had a single-point wear rate

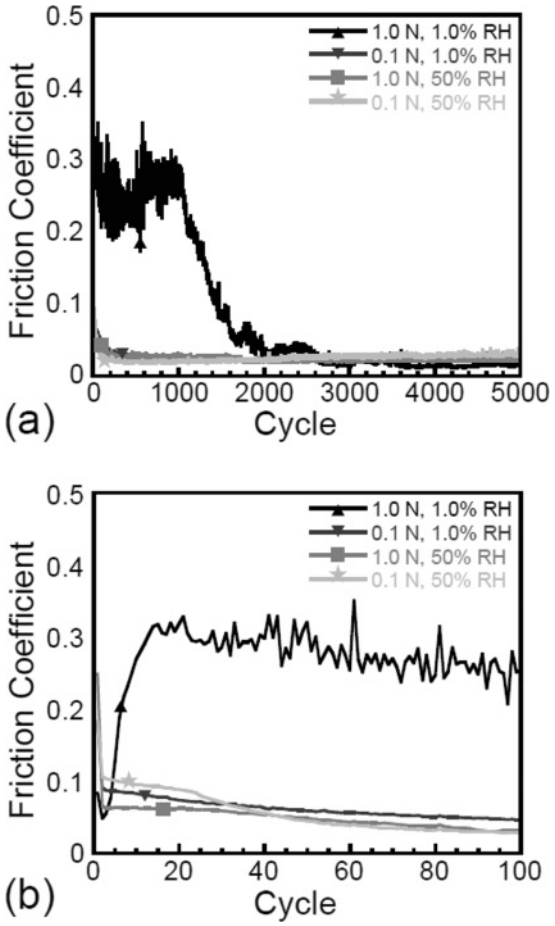

FIG. 4. (a) Friction plot for self-mated UNCD RH/load study. (b) Zoom of first 100 cycles to highlight high-friction behavior for 1.0% RH track. All tracks were run for 5000 total cycles.

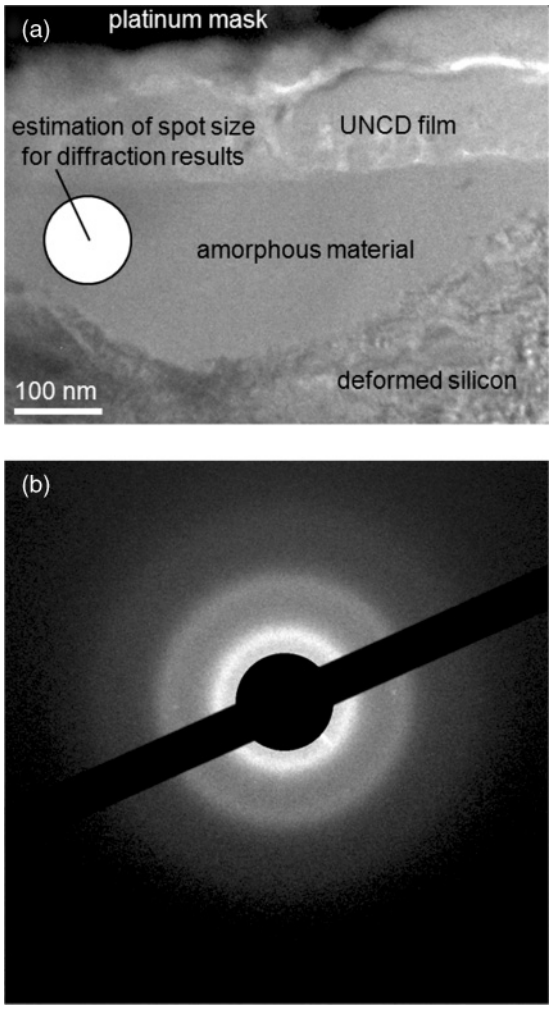

FIG. 5. (a) TEM image from a cross-section of the 1.0 N, 1.0% RH UNCD wear track. (b) Diffraction pattern from the highlighted region in (a) showing complete lack of ordered silicon crystalline structure.

of 9.7×10^{-7} $mm^3N^{-1}m^{-1}$. The 0.5 N, 1.0% RH ta-C track experienced severe plastic deformation of the substrate, as did the UNCD tracks made at 1.0% and 2.5% with a 1.0 N load. For the 1.0 N UNCD studies, the initial mean contact pressure (assuming a Hertzian model with a Si_3N_4 sphere, radius 1.5 mm, 250 GPa modulus, and 0.24 Poisson ratio contacting a Si flat with 160 GPa modulus, and 0.245 Poisson ratio) was 649 MPa, with a contact diameter of 44.3 μm. The final average contact pressures for the UNCD tracks, calculated from the measured width of each wear scar, were 40.6 MPa, 44.6 MPa, 757.0 MPa, and 6.5 GPa for 1.0% RH, 2.5% RH, 5.0% RH, and 50.0% RH, respectively. Using the same Hertzian model, the 0.5 N ta-C interface started at 517 MPa mean Hertzian contact pressure with a 35.1 μm contact diameter. The final contact pressures were 26.5, 78.6, 196.0, and 329.0 MPa for 1.0% RH, 2.5% RH, 5.0% RH, and 50.0% RH, respectively. The values for UNCD suggest that either the effective modulus was higher due to contributions from the film (UNCD having a much higher modulus than Si or Si_3N_4), or that the local roughness affected the geometry of the contact. These films are thin (1–2 μm), and they have high strength compared to the underlying Si substrate. A transmission electron microscope (TEM) cross section for the 1.0 N, 1.0% RH UNCD track (see Fig. 5) revealed that, even though the track was 4 μm deep and the Si substrate had undergone an amorphous phase change, there was still a UNCD film on top of the amorphous Si inside the track. The NEXAFS spectroscopy confirmed the presence of UNCD coatings within all wear tracks. As mentioned previously, the wear of the load/RH UNCD tracks was discussed elsewhere.[13]

Raman spectroscopy measurements confirmed that both carbon films remained in the worn portions of every sphere, and the spectra were qualitatively similar when comparing worn and unworn areas. These measurements are helpful since PEEM can not be used to characterize the chemistry of the spheres due to their nonplanar geometry (alternate methods, at lower spatial resolution, can be used for x-ray absorption studies of nonplanar samples[21]). Raman spectra were not acquired on the flats.

Analysis of the *ex situ* PEEM data reveals information about the tribochemical reactions that occurred due to the tribological conditions during testing. Figure 6(a) is a PEEM image obtained at 289.0 eV from the 0.5 N, 1.0% RH ta-C track. The image shown has a region of interest (ROI) indicated within the wear-track borders. The bottom spectrum (light grey) shown in Fig. 6(b) is a reference taken on an unworn

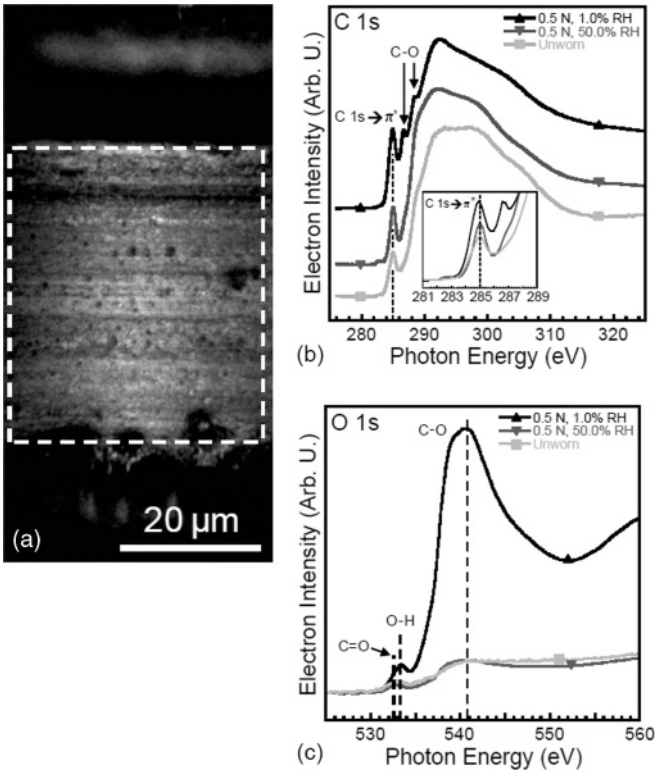

FIG. 6. (a) ta-C PEEM image taken with 289.0 eV photons on heavily worn (0.5 N, 1.0% RH) wear track, (b) carbon 1*s* spectra from heavily worn, lightly worn, and unworn parts of the sample (heavily worn ROI shown in image), (c) corresponding oxygen 1*s* data [same ROIs as in (b)].

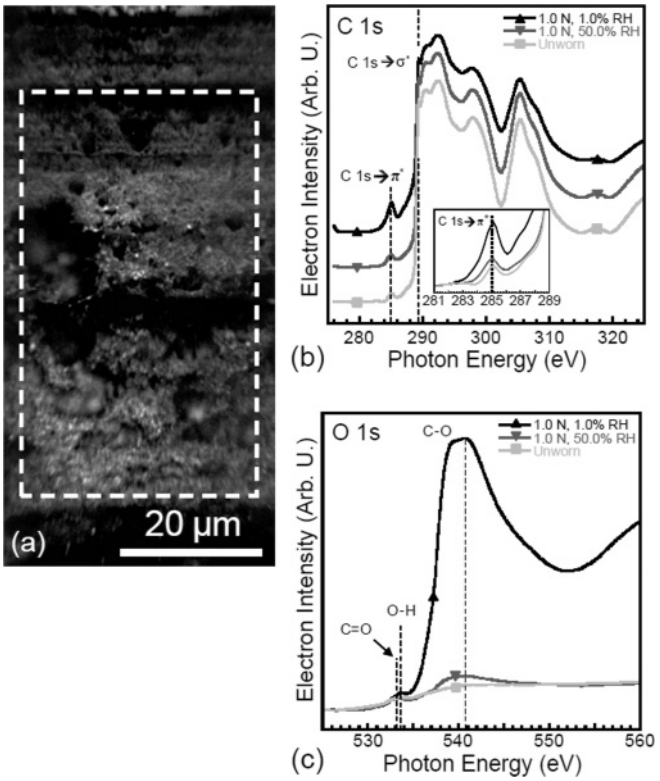

FIG. 7. (a) UNCD PEEM image taken with 289.0 eV photons on heavily worn (1.0 N, 1.0% RH) wear track, (b) carbon 1*s* spectra from heavily worn, lightly worn, and unworn parts of the sample (heavily worn corresponds to ROI in image), (c) corresponding oxygen 1*s* spectra [same ROIs as in (b)].

portion of the ta-C sample, and the top spectrum (black) is from the worn region in Fig. 6(a). The middle spectrum (dark grey) is from the 0.5 N, 50.0% RH track, which, as discussed above, was only lightly worn (PEEM image not shown). Carbon 1*s* spectra for ta-C have two predominant identifying features. The first is a peak at 285.0 eV due to the C $1s \rightarrow \pi^*$ transition. This reflects the presence of disordered carbon-carbon double bonds (π bonds). The second is a broad feature due to the C $1s \rightarrow \sigma^*$ transition that begins at ~289.0 eV, which arises from the σ bonding present in both disordered carbon-carbon single and double bonds. Since ta-C is amorphous and contains a range of bond lengths, the C 1*s* NEXAFS spectra lack any sharp post-edge resonances.

There are two main spectroscopic differences between the heavily-worn (0.5 N, 1.0% RH) and unworn ta–C spectra. The first is the increase in the C $1s \rightarrow \pi^*$ peak at 285.0 eV for the 1.0% RH track. The second is the significant amount of oxidation in the wear track, as evidenced by the peaks in the heavily worn C 1s spectrum at ~286.7 and ~288.6 eV, which are assigned to a C-O Rydberg orbital and C-O σ^* antibonding orbital, respectively.[38] The spectrum from the lightly worn 0.5 N, 50.0% RH track (dark grey) shows some increase in the C $1s \rightarrow \pi^*$ peak at 285.0 eV, giving evidence of a small amount of rehybridization, and some traces of oxidation.

The oxygen 1*s* spectra [see Fig. 6(c)] also highlight the differences between the three regions. The spectrum from the unworn area (light grey) and the spectrum from the 0.5 N, 50.0% RH track (dark grey) are similar in both shape and intensity. There is a small peak at 532.7 eV corresponding to a π^* transition for double-bonded oxygen,[39] and then a low, broad hump starting at 538.0 eV, which is due to the σ component of single- and double-bonded oxygen. The unworn spectrum has a low overall intensity, and would not be expected to reveal the presence of a large amount of oxygen. The relative intensities of these two curves indicate that there is little oxygen in the 0.5 N, 50.0% RH track. In the case of the 0.5 N, 1.0% RH track (black spectrum), there is substantially more oxygen overall as noted by the much higher intensity of the entire spectrum. The intensity at 541.0 eV is almost eight times higher for the 0.5 N, 1.0% RH track than for the other two spectra. Furthermore, the oxygen is more σ bonded as opposed to π bonded, as demonstrated by the much larger edge jump at 538.0 eV and the noticeable C-O feature at ~541 eV. As well, for the 0.5 N, 1.0% track, there is a small but detectible shift in the pre-edge peak to 533.4 eV, which corresponds to the presence of an O-H bond.[38]

The PEEM results from the UNCD constant-load study are similar to those from the ta-C constant-load study. Figure 7(a) is a PEEM image taken at 289.0 eV from the UNCD track created at 1.0 N, 1.0% RH (also discussed previously[13]). This image is from a region entirely inside the borders of the wear track. The bottom spectrum (light grey) in Fig. 7(b) is from an unworn portion of the same UNCD sample. The peak at 285.0 eV is due to the C $1s \rightarrow \pi^*$ transition for disordered carbon-carbon bonds. This peak directly correlates with the amount of sp^2-bonded carbon in the sampled region, which is

due to the grain boundaries, surface contamination, and surface reconstruction (~2–5% initially, as in all UNCD films). The edge jump at ~289.0 eV, the exciton peak at ~289.3 eV, and the second band gap at 302.5 eV are all features of the C $1s \rightarrow \sigma^*$ transition for ordered sp^3-hybridized carbon-carbon bonds. The top spectrum (black) in Fig. 7(b) is from the ROI in Fig. 7(a). The spectrum from the 1.0 N, 1.0% RH track shows evidence of both $sp^3 \rightarrow sp^2$ rehybridization of the carbon bonds (i.e., an increase in peak height at 285.0 eV) as well as oxidation (features at ~286.4 and ~288.6 eV). Figure 7(c) shows that the UNCD oxygen data are very similar to the ta-C data. There is a weak oxygen signal from the unworn portion of the sample (light grey spectrum), with the 1.0 N, 50% RH track (dark grey spectrum) having only 37% more intensity at 541.0 eV than the unworn spectrum. The small, broad pre-edge feature is centered at 533.2 eV, and is attributed to an overlap of peaks from the π-bonded oxygen as well as hydroxyl groups. The broad feature starting at 538.0 eV is from the σ-bonded oxygen. These spectra contrast starkly with the significant oxygen seen in the 1.0 N, 1.0% track (black spectrum). The intensity is nearly eleven times higher for the 1.0% track compared to the unworn spectrum. Here the pre-edge peak is centered at 533.5 eV, which, like ta-C, indicates more O-H bonding. The edge jump is apparent at 538.0 eV, with a C-O feature at 541.0 eV.

IV. DISCUSSION

The results demonstrate that the tribological behavior of ta-C and UNCD are strongly controlled by both the RH in the environment and applied load. The RH determines the amount of water vapor that is available to interact with the surfaces, which affects the tribochemistry. The load (related to contact pressure) influences the normal and shear stresses at the contact, and these stresses will govern the amount of bond breaking during sliding contact.

A. Overview of lubrication mechanisms

It has been previously hypothesized that lubrication of diamond or other highly sp^3-bonded carbon-based materials could occur by either: (1) rehybridization of the carbon bonds on the surface to form a "graphitic" layer, a mechanism which should be independent of RH (oxidation only affects rehybridization of diamond at temperatures above 600 °C) and would be manifested as a significant change in the sp^2 character of all surfaces that achieve low friction,[30,40,41] or (2) passivation of dangling bonds produced during sliding by species from the ambient environment, which would depend on the amount of RH available to react within the contact.[17,42]

Based on the tribometric and spectroscopic evidence, we propose that the primary lubrication mechanism for both ta-C and UNCD is passivation of dangling bonds by dissociated water species, and not graphitization or rehybridization of the surface carbon bonds.[13] The spectroscopic evidence that refutes the hypothesis that graphite is formed even in the harshest wear conditions (low RH, high load) is shown in the heavily worn spectra in Figs. 6(b) and 7(b). Among several other distinct and specific features, ordered graphite displays a shift in the NEXAFS C $1s \rightarrow \pi^*$ feature from 285.0 eV for

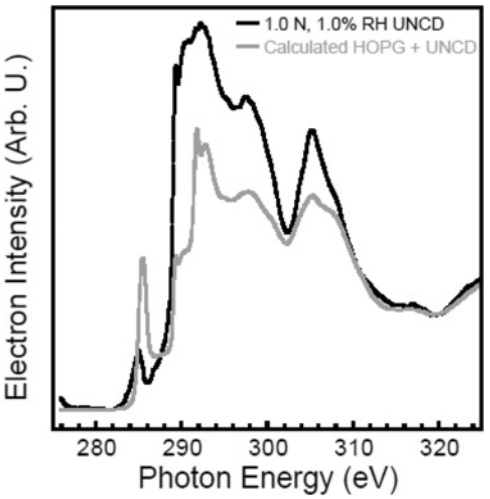

FIG. 8. NEXAFS spectrum from the 1.0 N, 1.0% RH UNCD track (black) and the calculated spectrum for one monolayer of graphite on top of UNCD (gray).

disordered sp^2 bonds to 285.5 eV for graphite.[13,33,43] This shift is well within the energy resolution of our NEXAFS spectroscopy. None of the spectra from any of the wear tracks show a shift in the C $1s \rightarrow \pi^*$ transition, indicating there is no detectible graphite. Furthermore, as discussed elsewhere,[13] a simulated NEXAFS spectrum constructed for a layer of graphite on top of UNCD failed to match the experimentally observed spectra. That calculation used a highly ordered pyrolytic graphite (HOPG) spectrum separately obtained with photons incident at the "magic angle" (54.7° from the surface normal, meaning the polarization vector was at 35.3° from the surface normal). However, in the PEEM system used in this work, the polarization vector of the light is always parallel to the sample surface. This changes the strength of the interaction between the x-ray polarization and the surface bonds. An improved calculation is shown in Fig. 8. The HOPG spectrum used in the summation was obtained on the same PEEM system (meaning the polarization is identical for all measurements in this manuscript), and the weighting of the spectra based on relative thickness accounts for the angle of incidence of the light (which is 60° from the surface normal). As before, the calculation is for UNCD covered with a thin layer of HOPG having an assumed thickness of 0.335 nm (the interlayer spacing of graphite), making the effective x-ray sampling depth $0.335/\cos(60°) = 0.67$ nm for the graphite layer. Comparing this calculated spectrum to the spectrum from the 1.0 N, 1.0% RH UNCD track, it is still immediately apparent that there is no evidence for graphite formed on the surface of the UNCD track even at the level of one monolayer. As before,[13] there is no detectible shift of the C $1s \rightarrow \pi^*$ peak from 285.0 to 285.5 eV in the experimental result for UNCD, which indicates the absence of ordered, graphitic carbon. Also different are the σ^* excitonic features for graphite, which show strong absorption at ~292 eV. These features do not show up in any of the C $1s$ spectra taken from either UNCD or ta-C. This assumes graphite is lying flat on the wear track. However, NEXAFS of graphite at an angle such that the π orbitals were more strongly excited by the x-rays would

show a more increased peak at ~285 eV, while still retaining some of intensity from the graphite σ^* features at ~292 eV. Regardless, the spectrum would look noticeably altered from the UNCD spectrum, and this is not seen. Using the slightly different NEXAFS spectrum of graphene would lead to the same conclusion.[44]

However, oxidation occurs in all cases (small amounts for tracks with low wear, and significant oxidation for cases of high wear) as shown in the O 1*s* spectra in Figs. 6(c) and 7(c). The mechanism leading to oxidation is proposed as follows. As surface bonds are broken in the sliding contact, dangling carbon bonds will be exposed. Some of these bonds will be subsequently passivated by dissociated water in the form of -H and -OH groups. The number of broken bonds per pass will be determined by the surface structure at the interface and the contact stresses, and the number of bonds passivated per pass will be determined by the RH level. For reference, at 1.0% RH and ambient temperature, the impingement rate of water molecules to the surface is 9.6×10^{17} $cm^{-2}s^{-1}$. For an unterminated diamond (111) surface, assuming that every H_2O dissociates into OH and H with a sticking coefficient of 1, it would take 2.5×10^{-5} seconds to become fully passivated. In this way, the friction state of the system depends on a balance between bond breaking and bond passivation.

B. Role of carbon rehybridization

While neither film shows evidence of graphitization, there is some degree of rehybridization ($sp^3 \rightarrow sp^2$ conversion). This is seen in the NEXAFS spectra as an increase in the C $1s \rightarrow \pi^*$ feature at 285.0 eV [see Figs. 6(b) and 7(b)]. This happens for both films, with a greater amount of rehybridization for tracks with higher friction and wear (i.e., for higher loads and lower RH levels). UNCD films, as grown, have an sp^2 fraction of ~2–5% (located at grain boundaries). The most heavily modified region of the most severely worn UNCD track (1.0 N, 1.0% RH) has an sp^2 fraction of ~20%, with the average over the entire analyzed PEEM region being ~18%. For the most severely worn ta-C track (0.5 N, 1.0%), the peak height of the C $1s \rightarrow \pi^*$ feature increases in intensity by 84%. This peak height is related to the amount of sp^2-bonded carbon, but the amount of sp^2 bonding cannot be quantified without a detailed calculation of the spectra or an independent calibration using a technique such as NMR.[32,45] Regardless, it shows that rehybridization has taken place.

However, the data suggest that the conversion from sp^3- to disordered sp^2-bonded carbon is not the primary lubrication mechanism, and may not contribute significantly to lubrication at all. First, for the ta-C and UNCD constant-load studies, tracks from the same film after run-in have the same friction coefficient, though they have very different levels of amorphous carbon. This shows that the carbon rehybridization, in the range experienced by the ta-C and UNCD tracks that ran in, has no correlation with the friction coefficient. Indeed, while some studies have suggested that polycrystalline diamond films with increased sp^2 fractions exhibit lower friction and wear by making films more lubricious,[15] other work showed amorphous H-free carbon-based films with more sp^2 content have poorer tribological properties.[46,47] As well, the steady-state friction for ta-C, despite having more sp^2-bonded carbon, is always higher than for UNCD, even under less-harsh conditions (lower load, higher RH). Also, more sp^2-bonded carbon tends to render films more reactive, and to reduce the modulus and hardness.[48] Based on this, there is no reason to expect that sliding-induced conversion of carbon to disordered sp^2 hybridization lowers friction, and in some cases will actually increase the friction if there are dangling bonds that interact with the counterface.[49] The rehybridization may simply occur as an inevitable side-effect of bond breaking during the complex interactions and atomic rearrangements induced by high stresses during sliding.

The results from the 0.5 N, 1.0% RH ta-C track, which did not run in to a low steady-state friction coefficient, provide insight into the differences between ta-C and UNCD. Even though the constant-load ta-C tracks were created using a lower applied load than that used for the constant-load UNCD tracks (0.5 N for ta-C, 1.0 N for UNCD), the 1.0 N, 1.0% RH UNCD track eventually achieved low friction while the 0.5 N, 1.0% RH ta-C track did not (see Figs. 1 and 2, or 3 and 4, and Table I). Although the contact pressure for the 0.5 N, 1.0% RH ta-C track reduced as the track width grew, the pressure apparently remained high enough throughout the duration of the test such that the dangling bonds formed during sliding contact were unable to be passivated sufficiently rapidly by the ambient species. For these tracks, the final average contact pressure for UNCD was 53% higher than that for ta-C (40.6 versus 26.5 MPa), yet the UNCD was still able to obtain low friction at 1.0% RH. Furthermore, for the load/RH study, it was desirable to cover an order of magnitude change in load. The highest applied load for the ta-C tests was limited at 0.5 N because higher loads led to strong adhesion and insurmountable static friction between the sphere and the sample. UNCD films were able to sustain a higher initial load (1.0 N) without such adhesion and friction.

There are several material properties, some of which are interrelated, that could contribute to this different tribological behavior of ta-C and UNCD at low RH. One factor is the respective sp^2 fraction of each film. While materials comprised of doubly bonded carbon can be good solid lubricants (e.g., graphite[50] and hydrogenated diamond-like carbon[22,24]), double bonds are typically more chemically reactive and mechanically unstable than single bonds. Therefore such species are more likely to engage in tribochemical reactions that lead to bond breaking and subsequent bond formation across the interface. This is consistent with reactive molecular dynamics simulations of the sliding of amorphous carbon films.[25] Because of this, a material with a higher percentage of sp^2 bonds may need a higher amount of passivating species in the environment to passivate the dangling bonds before they form a bridge across the interface. Another possible cause is the difference in surface roughness. The fact that ta-C is smoother than UNCD means that the true contact area for ta-C self-mated interfaces is closer to the apparent (Hertzian) contact area. The somewhat lower Young's modulus of ta-C will also lead to a higher true contact area. Since the friction depends on the true contact area, a significantly higher contact area will mean higher friction and more intimate contact leading to the opportunity for bonds to form across the interface, as discussed for hydrogenated carbon films.[51] A detailed analysis of the roughness would be required to further explore how different

the contact areas are for UNCD and ta-C samples, both initially and as they wear.

C. Oxidation under low and high friction

For the tracks made at higher humidities (which run in quickly and have low wear), NEXAFS data reveal that their chemical states are nearly identical to regions outside the wear track, differing only due to a slight amount of oxidation within the 50.0% wear tracks (dark grey spectra in Fig. 6(c) for ta-C, Fig. 7(c) for UNCD). The intensity is the same for the O 1*s* peak at 541.0 eV for the 0.5 N, 50.0% ta-C track and the unworn region, and is only 37% higher for the 1.0 N, 50.0% UNCD track compared to the unworn region. The observations of low wear and minor changes in surface chemistry imply that a finite but small number of bonds are broken during sliding and then passivated by both -H and -OH groups. This is most likely to occur during the first few cycles when friction is highest.

However, the ta-C and UNCD tracks made at lower humidities (which exhibit longer run-in periods and higher wear), undergo significant chemical changes. Along with some rehybridization of surface carbon bonds discussed above, the oxygen NEXAFS data reveal a significant increase in the amount of oxidation. Furthermore, Figs. 6(c) and 7(c) show that O atoms primarily form σ (538 eV and above) and not π (532.7 eV) bonds. This suggests that there is a single dominant oxidation mechanism that occurs during wear, namely that hydroxyl groups bond to the surface in the form of C-OH groups.[38] The O 1*s* spectra would also be consistent with the formation of ester (C-O-C) groups; however, forming these requires extra bond-breaking steps (breaking the O-H bond formed after dissociative adsorption of H_2O, then bonding of the unbonded O radical with a nearby carbon radical). In Sec. IV G, we discuss theoretical studies that support the formation of $-$OH groups on the surface. Note that H, expected from the dissociative adsorption of water, is still anticipated to form C-H, but the C-H $1s \rightarrow \sigma^*$ resonance at 287.5 eV is difficult to resolve and compare between spectra from different regions.

The oxidation is seen, for example, in the case of the 1.0 N, 1.0% RH UNCD track, where low friction was achieved after a 2660 cycle run-in period (Figs. 1 or 3), and the surface oxygen exhibited predominant $1s \rightarrow \sigma^*$ character [see Fig. 7(c)]. In contrast, the 0.5 N, 1.0% RH ta-C track never achieved low friction, so the high level of oxidation could have either occurred during the test (although at a level insufficient to fully passivate the surface) or after the test was complete (if dangling bonds were still present upon completion of the test), or through both means. Regardless, the chemical evidence suggests that these worn surfaces were driven toward a state with an increased amount of sp^2 bonding and C-OH bonding due to sliding.

D. Factors controlling run-in behavior

Previous polycrystalline diamond run-in studies involved modification of the surface morphology and chemistry prior to testing by polishing[31] or changing the film growth conditions.[15] Here, we establish that the run-in behavior for self-mated interfaces of both UNCD and ta-C can be controlled by only varying environmental conditions during sliding. For all systems studied here, when the load is held constant, increasing the RH level decreases the number of run-in cycles. This demonstrates the important role that tribochemistry plays in the conditioning of these hard carbon-based interfaces, consistent with results described previously[13] establishing that the formation and passivation of dangling carbon bonds during sliding is largely responsible for the friction and wear performance of ta-C and UNCD.

In the present experiments, for a given material and a given load, the initial mean contact pressure is a fixed value regardless of RH. As sliding begins, there is similar friction behavior for the first few cycles in different RH environments [highlighted for ta-C in Fig. 1(b)]. Subsequently, each system evolves differently depending on whether or not the bonds that are broken during sliding are able to be passivated sufficiently quickly. Profilometry on all ta-C and UNCD tracks created at higher humidities ($> 2.5\,\%$) show low wear and low track widths, meaning lower apparent contact areas and therefore higher average contact pressures. PEEM studies for the 50.0% RH tracks made at the low or high load, for either film, reveal that the chemical state is almost identical to that of the respective unworn film with only a small amount of oxidation, indicating a steady-state sliding condition was achieved. Specifically, the run-in process wore down the highest asperities (which are the locations that produce the highest contact stresses), the dangling bonds formed during this wear were passivated by -H and -OH groups, and the new larger contact area leads to a lower contact pressure and consequently a low amount of further bond breaking. In other words, the interface is "self-stabilizing."

The UNCD and ta-C tracks created at 1.0% RH with 1.0 N and 0.5 N loads, respectively, behave very differently (see Figs. 1 and 2, or 3 and 4, and Table I). As sliding begins, there are not enough passivating species in the environment to terminate the dangling bonds formed, and the resulting friction coefficients remain high (0.6 for ta-C, 0.25 for UNCD). The high friction is emblematic of the large number of bonds forming across the interface. This leads to a high wear rate of both the sphere and flat. The track width therefore grows and asperities are worn. This lowers both the average and the maximum local contact pressures. However, the ta-C interface under the 0.5 N load never recovers from this state, and has high, fluctuating friction for the entire 5000 cycles. A Fourier transform of this ta-C friction plot is featureless, suggesting the fluctuations simply come from the random occurrences of large numbers of bonds breaking and forming across the interface. Unlike ta-C, the UNCD track does reach a low-friction state, after 2660 cycles. However, the topography of this track was heavily modified from wear of the UNCD itself and from plastic deformation of the silicon substrate (see Fig. 5), both of which contributed to creating a larger contact area and thus lowering the contact pressure that likely helped lead to reduced friction. Regardless, in both cases, severe wear occurred with protracted run-in behavior, showing that the combined effects of high contact stress and low relative humidity inhibit the interface from "self-stabilizing" during sliding.

As discussed above, the NEXAFS results show that both tracks are heavily oxidized with predominantly σ-bonded

oxygen from the dissociative adsorption of water molecules, leading to -OH and -H species on the surfaces. In an environment with a relatively high partial pressure of water (50.0% RH), the system can accommodate a higher contact pressure (more bonds broken per unit sliding distance) if the flux of available impinging species is high enough to passivate the dangling bonds within the exposure time between sliding passes. However, as the partial pressure of water in the system is lowered, low friction can only be maintained at lower contact pressure (meaning fewer broken bonds per sliding distance). The transition between high and low friction can be understood as the transition in the critical value of number of broken bonds formed per sliding pass versus the number of bonds passivated between wear events.

E. The variable degree of oxidation needed for low friction

Low steady-state friction can be achieved for conditions where there is both low and high degrees of oxidation. For example, all UNCD tests from the constant-load study achieved similar steady-state friction coefficients of ∼0.01–0.02 regardless of their level of oxidation. The 1.0 N, 1.0% RH UNCD track exhibited a large amount of σ-bonded oxygen [see Fig. 7(c), black spectrum], while the other UNCD tracks exhibited far less oxygen overall and exhibited a mixture of C=O and C-O bonding [see Fig. 7(c), dark grey spectrum]. In addition, the low-load tracks for both ta-C and UNCD at 50.0% RH show nearly the same intensity of oxygen as the unworn spectra from the respective samples. Those spectra also have the same line shapes, which show a mixture of π- and σ-bonded oxygen. These relative and absolute amounts of C-O bonding give insight into the UNCD wear history (similar to what was seen for ta-C, although low friction was not achieved under the most severe conditions). The tribometry for UNCD shows that the oxidation state does not affect the steady-state friction behavior. This indicates that ta-C and UNCD are best tribologically either in conditions where very few surface bonds are broken during sliding (i.e., the surface remains mostly identical to the as-deposited surface), or in conditions where broken bonds are passivated with species dissociated from water, which in this case are hydroxyl and hydride groups (or possibly other singly bonded oxygen groups such as ether groups, discussed further below).

F. Effects related to load

If passivation is the lubrication mechanism, then the load should also affect the friction performance since it will change the interfacial contact stresses which in turn affect bond breaking. This effect is most noticeable at lower humidity. Lowering the load from 0.5 N to 0.05 N at 1.0% RH for ta-C (see Fig. 3) changes the behavior from not running in at all to running in within 150 cycles. This effect was also seen for the UNCD load/RH study, where changing the load between 1.0 N and 0.1 N at 1.0% RH greatly reduced the number of cycles needed for run-in (see Figs. 4(a) and 4(b) and Table I).

However, at 50.0% RH, for both ta-C and UNCD, there is only a modest dependence of the friction coefficient on load. Furthermore, the friction coefficient is actually higher for the lower load experiments at 50% RH. For example, for ta-C, the steady-state friction coefficient for the 0.5 N, 50.0% RH test was ∼0.05 (see Fig. 1 or 3 and Table I). This is less than half the value of the steady-state friction for the 0.05 N tracks at both 1.0% and 50.0% RH (see Fig. 3, Table I). This effect is well understood from other studies of highly conforming solid lubricants interfaces[52] as resulting from the reduced Hertzian contact pressures at lower loads, leading to a higher ratio of true contact area (and thus friction) to the applied load. This can be explained by considering that the friction force is directly proportional to the true contact area, and that the contact area is a sublinear function of the normal force, even for somewhat rough interfaces.[53] Although reducing the normal load decreases the contact area, and thereby decreases the friction force, in this range the ratio of friction force to normal force (i.e., the friction coefficient) increases. The effect for ta-C is a factor of two increase in the friction coefficient for an order of magnitude decrease of the load. Similarly, it can be clearly seen in Fig. 1(a) that the friction coefficients for ta-C show a noticeable increase at increasing numbers of cycles. As the sphere and track wear, the average contact pressures reduce, and the ratio of true contact area (and thus friction force) to load increases. This leads to a higher friction coefficient.

In summary, with a sufficient amount of passivating species in the environment to enable run-in to a steady, passivated state, other properties of the interface such as surface roughness, true contact area, contact stresses, and material stiffness and strength (i.e., resistance to elastic deformation and bond breaking) are interrelated, determining factors for the initial friction coefficient and run-in behavior.

G. Theoretical support for passivation mechanism

The dissociative adsorption of water molecules on diamond surfaces with dangling bonds to form hydride and hydroxyl terminations is supported by *ab initio* density functional theory (DFT) calculations. Zilibotti *et al.*[54] calculated the equilibrium energies of diamond surfaces passivated with H_2O, H_2, and O_2, and Manelli *et al.*[55] calculated kinetic barriers and equilibrium energies for both molecular physisorption and dissociative chemisorption of water on diamond (001) surfaces. Together, these studies show highly favorable adsorption energies for both physisorption (0.21–0.43 eV/molecule) and dissociative chemisorption of water (1.7–3.9 eV/molecule), producing passivated diamond surfaces with low surface energy and low self-mated works of adhesion. They also show that as the concentration of H_2O increases, the formation of a surface involving both hydride and hydroxyl terminations is favorable.[54] Similarly, DFT applied by Qi *et al.*[56] showed that breaking one of the O-H bonds in water and then passivating two carbon atoms with the resultant H and OH groups has an adsorption energy of 1.8 eV/molecule. Overwhelmingly, the DFT work concludes that the dissociative adsorption of H_2O to form C-H and C-OH groups on the surface is expected.

The spectroscopic evidence from the oxygen NEXAFS spectra [see Figs. 6(c) and 7(c)] is consistent with the hypothesis that the surface has been partially passivated with hydroxyl groups, since the observed CO bonding is primarily of a sigma nature in the heavily worn tracks where significant numbers of

bonds have been broken. The spectra provide little evidence for the presence of increased C=O bonding, and are consistent with the formation of C-OH bonds. The spectra alone do not allow us to rule out C-O-C bonding. However, starting with an unpassivated diamond surface exposed to molecular water vapor, achieving a C-O-C-terminated surface is a more complex process than the formation of the hydroxylated (or hydroxylated and hydrogenated) surface. Thus the simpler process of hydroxylation is naturally expected to predominate. This also is supported by the DFT calculations of Zilibotti *et al.*[54] who found that a fully etherized surface is energetically unfavorable with respect to the unterminated diamond (001) 2×1 surface.

There is additional spectroscopic evidence in our study strongly suggesting the presence of hydroxyl groups on the surface. First, the polarization of the synchrotron radiation is parallel to the plane of the sample surface. For hydroxyl groups that are oriented nearly normal to the surface, the orbital direction for all of the σ bonds (both C-O and O-H bonds) would also be normal to the surface. Thus there would be weak coupling between the photon polarization direction and the orbital direction. The C 1*s* and O 1*s* NEXAFS data in this study all show weak σ features related to the C-O and O-H bonding expected for hydroxyl groups ($\sim$286.7 and 288.6 eV for carbon, $\sim$533.5 eV for oxygen). If there was a significant amount of C=O bonding, with the bond direction still oriented mostly normal to the surface, the polarized photons would interact strongly with the π orbitals and intense peaks would be seen in the spectra, especially in the O 1*s* spectrum at $\sim$532 eV. The large intensity of the σ features in the O 1*s* spectra are due to some type of C-O bonding, likely here in the form of C-OH bonds.

Zilibotti *et al.* also showed that surfaces that were H- or OH-terminated had low self-mated works of adhesion.[54] This agrees well with MD work by Gao *et al.*,[25] which showed that friction and adhesion are low for hydrogen-terminated diamond surfaces, but friction goes up as hydrogen is removed from the surface. These results support the argument that hydroxylated diamond surfaces will reduce attractive interactions across an interface, which should in turn reduce bond formation across the interface, thus reducing friction and wear. In an environment with fewer passivating species available, this would be crucial since lower friction would mean fewer bonds broken per sliding pass, leading to fewer dangling bonds needing passivation.

V. CONCLUSION

This work presents the self-mated tribological behavior of ta-C and UNCD, two ultrahard, nearly H-free, highly sp^3-bonded carbon films as a function of load and RH in dry argon. These are the first tribological studies characterized by PEEM-NEXAFS for ta-C. The overarching conclusion is that ta-C, similarly to UNCD,[13] is lubricated by passivation of the surface dangling bonds by dissociated water vapor. In other words, sliding inevitably produces dangling bonds, but the overall tribological behavior is predominantly governed by the competition between the subsequent formations of bonds across the interface versus the passivation of the dangling bonds by the dissociative adsorption of water. While there is some rehybridization of sp^3-bonded carbon to sp^2 bonding, there is no evidence for the formation of ordered graphitic carbon. Furthermore, amorphous rehybridization alone is not itself a known mechanism of solid lubrication and, even under the harshest conditions, the most strongly rehybridized regions of the UNCD wear tracks only exhibit a 15% increase in sp^2 bonding (from 5% to $\sim$20%). Rather, the key to low friction and low wear is either maintaining a high degree of passivation via the original inert hydride termination, or sufficiently passivating any dangling bonds produced with dissociated vapor species.

With a constant load, both ta-C and UNCD show a trend of increasing number of run-in cycles with decreasing RH. This demonstrates that the run-in behavior, or in other words the rate at which the interface will reach steady state, is determined by the vapor environment during sliding. The spectroscopic results show that there is a distinct trend in the type and quantity of oxygen bonding in both the ta-C and UNCD wear tracks created at different RH levels. Tests at successively lower RH levels have increasingly higher amounts of oxygen bonded in the track. The oxygen bonding is always more σ than π bonded, consistent with hydroxyl bonding. In contrast, tracks created in higher-RH environments show only slight oxidation compared with areas unmodified by wear. The tracks created at the lowest RH (1.0%) are also the ones that have highest friction initially, and higher total wear. For ta-C, which has a larger fraction of sp^2-bonded carbon (as-grown), a smoother surface, and a lower modulus and hardness compared with UNCD, friction is higher and is more environmentally sensitive than for UNCD. Our results suggest that low friction and wear are not due to an increase in sp^2 content. Finally, the dependence of the tribochemistry on the contact pressure and environment is what determines the tribological performance. Excessively high loads and insufficient quantities of passivating vapor species (water, in the case studied here) lead to poor performance; however, the threshold values for these quantities are impressive (e.g., self-mated interfaces of ta-C and UNCD still exhibit excellent tribological behavior under rather harsh conditions, with $>$500 MPa mean contact pressures and RH as low as 2.5%), suggesting a wide range of applications for such materials.

ACKNOWLEDGMENTS

We thank A. Schöll and A. Doran for their help with PEEM measurements. Funding was provided by Air Force grant FA9550-08-1-0024. This research was partially supported by the Nano/Bio Interface Center through the National Science Foundation NSEC DMR08-32802. The Advanced Light Source is supported by the Director, Office of Science, Office of Basic Energy Sciences, of the US Department of Energy under Contract No. DE-AC02-05CH11231. This research was supported in part by the Sandia National Laboratories, sponsored by Sandia Corporation (a wholly owned subsidiary of Lockheed Martin Corporation) as Operator of Sandia National Laboratories under its US Department of Energy Contract No. DE-AC04-94AL85000. Use of the Center for Nanoscale Materials was supported by the US Department of Energy, Office of Science, Office of Basic Energy Sciences, under Contract No. DE-AC02-06CH11357.

*Currently at the National Institute of Standards and Technology

[1] A. V. Sumant, D. S. Grierson, J. E. Gerbi, J. Birrell, U. D. Lanke, O. Auciello, J. A. Carlisle, and R. W. Carpick, Adv. Mater. **17**, 1039 (2005).

[2] D. H. Lowndes, V. I. Merkulov, A. A. Puretzky, D. B. Geohegan, G. E. Jellison, C. M. Rouleau, and T. Thundat, *Amorphous Diamond Films Deposited by Pulsed Laser Ablation: The Optimum Carbon-ion Kinetic Energy and Effects of Laser Wavelength*, edited by R. K. Singh, D. H. Lowndes, D. B. Chrisey, E. Fogarassy, and J. Narayan, Vol. 526 (Mater. Res. Soc, San Francisco, CA, USA, 1998), p. 325.

[3] X. Shi, D. Flynn, B. K. Tay, S. Prawer, K. W. Nugent, S. R. P. Silva, Y. Lifshitz, and W. I. Milne, Philos. Mag. B **76**, 351 (1997).

[4] A. C. Ferrari, J. Robertson, M. G. Beghi, C. E. Bottani, R. Ferulano, and R. Pastorelli, Appl. Phys. Lett. **75**, 1893 (1999).

[5] H. D. Espinosa, B. C. Prorok, B. Peng, K. H. Kim, N. Moldovan, O. Auciello, J. A. Carlisle, D. M. Gruen, and D. C. Mancini, Exp. Mech. **43**, 256 (2003).

[6] H. J. McSkimin and P. Andreatch, Jr., J. Appl. Phys. **43**, 2944 (1972).

[7] J. Liu *et al.*, Small **6**, 1140 (2010).

[8] K. H. Kim, N. Moldovan, C. Ke, H. D. Espinosa, X. Xiao, J. A. Carlisle, and O. Auciello, Small **1**, 866 (2005).

[9] S. Cho, I. Chasiotis, T. A. Friedmann, and J. P. Sullivan, J. Micromech. Microeng. **15**, 728 (2005).

[10] K. Jonnalagadda, C. Sung Woo, I. Chasiotis, T. Friedmann, and J. Sullivan, J. Mech. Phys. Solids **56**, 388 (2008).

[11] A. V. Sumant, A. R. Krauss, D. M. Gruen, O. Auciello, A. Erdemir, M. Williams, A. F. Artiles, and W. Adams, Tribol. Trans. **48**, 24 (2005).

[12] C. Matta, O. L. Eryilmaz, M. I. De Barros Bouchet, A. Erdemir, J. M. Martin, and K. Nakayama, J. Phys. D: Appl. Phys. **42**, 075307 (2009).

[13] A. R. Konicek, D. S. Grierson, P. U. P. A. Gilbert, W. G. Sawyer, A. V. Sumant, and R. W. Carpick, Phys. Rev. Lett. **100**, 235502 (2008).

[14] D. S. Grierson *et al.*, J. Vac. Sci. Technol. B **25**, 1700 (2007).

[15] R. R. Chromik, A. L. Winfrey, J. Luning, R. J. Nemanich, and K. J. Wahl, Wear **265**, 477 (2008).

[16] C. Matta, M. I. De Barros Bouchet, T. Le-Mogne, B. Vachet, J. M. Martin, and T. Sagawa, Lubrication Sci. **20**, 137 (2008).

[17] M. N. Gardos and S. A. Gabelich, Tribol. Lett. **6**, 103 (1999).

[18] L. Joly-Pottuz, C. Matta, M. I. de Barros Bouchet, B. Vacher, J. M. Martin, and T. Sagawa, J. Appl. Phys. **102**, 1 (2007).

[19] M. A. Hamilton, A. R. Konicek, D. S. Grierson, A. V. Sumant, O. Auciello, W. G. Sawyer, and R. W. Carpick, in *STLE/ASME 2008 International Joint Tribology Conference, Miami, 2008* (ASME, 2008), p. 9.

[20] C. Matta, L. Joly-Pottuz, M. I. De Barros Bouchet, J. M. Martin, M. Kano, Z. Qing, and W. A. Goddard, III, Phys. Rev. B **78**, 085436 (2008).

[21] A. R. Konicek, C. Jaye, M. A. Hamilton, W. G. Sawyer, D. A. Fischer, and R. W. Carpick, Tribol. Lett. **44**, 99 (2011).

[22] J. Andersson, R. A. Erck, and A. Erdemir, Surf. Coat. Technol. **163-164**, 535 (2003).

[23] R. Prioli, M. Chhowalla, and F. L. Freire, Diam. Relat. Mater. **12**, 2195 (2003).

[24] O. L. Eryilmaz and A. Erdemir, Wear **265**, 244 (2008).

[25] G. T. Gao, P. T. Mikulski, and J. A. Harrison, J. Am. Chem. Soc. **124**, 7202 (2002).

[26] G. T. Gao, P. T. Mikulski, G. M. Chateauneuf, and J. A. Harrison, J. Phys. Chem. B **107**, 11082 (2003).

[27] J. A. Harrison, J. D. Schall, M. T. Knippenberg, G. T. Gao, and P. T. Mikulski, J. Phys.: Condens. Matter **20**, 354009 (2008).

[28] J. D. Schall, G. T. Gao, and J. A. Harrison, J. Phys. Chem. C **114**, 5321 (2010).

[29] J. A. Harrison, D. W. Brenner, C. T. White, and R. J. Colton, Thin Solid Films **206**, 213 (1991).

[30] A. Erdemir, G. R. Fenske, A. R. Krauss, D. M. Gruen, T. McCauley, and R. T. Csencsits, (Elsevier, Switzerland, 1999), p. 565.

[31] I. P. Hayward, I. L. Singer, and L. E. Seitzman, Wear **157**, 215 (1992).

[32] J. P. Sullivan, T. A. Friedmann, and A. G. Baca, J. Electron. Mater. **26**, 1021 (1997).

[33] D. S. Grierson, A. V. Sumant, A. R. Konicek, T. A. Friedmann, J. P. Sullivan, and R. W. Carpick, J. Appl. Phys. **107**, 033523 (2010).

[34] A. V. Sumant, D. S. Grierson, J. E. Gerbi, J. A. Carlisle, O. Auciello, and R. W. Carpick, Phys. Rev. B **76**, 235429 (2007).

[35] J. Birrell, J. E. Gerbi, O. Auciello, J. M. Gibson, J. Johnson, and J. A. Carlisle, Diam. Relat. Mater. **14**, 86 (2005).

[36] A. C. Rennie, P. L. Dickrell, and W. G. Sawyer, Tribol. Lett. **18**, 499 (2005).

[37] S. Anders *et al.*, Rev. Sci. Instrum. **70**, 3973 (1999).

[38] I. Ishii and A. P. Hitchcock, J. Electron Spectrosc. **46**, 55 (1988).

[39] S. G. Urquhart, A. P. Hitchcock, R. D. Priester, and E. G. Rightor, J. Polym. Sci., Part B: Polym. Phys. **33**, 1603 (1995).

[40] M. N. Gardos and B. L. Soriano, J. Mater. Res. **5**, 2599 (1990).

[41] S. E. Grillo and J. E. Field, J. Phys. D: Appl. Phys. **33**, 595 (2000).

[42] H. I. Kim, J. R. Lince, O. L. Eryilmaz, and A. Erdemir, Tribol. Lett. **21**, 53 (2006).

[43] S. Anders, J. Diaz, J. W. Ager, III, R. Y. Lo, and D. B. Bogy, Appl. Phys. Lett. **71**, 3367 (1997).

[44] D. Pacile, M. Papagno, A. F. Rodriguez, M. Grioni, L. Papagno, C. O. Girit, J. C. Meyer, G. E. Begtrup, and A. Zettl, Phys. Rev. Lett. **101**, 066806 (2008).

[45] T. M. Alam, T. A. Friedmann, P. A. Schultz, and D. Sebastiani, Phys. Rev. B **67**, 245309 (2003).

[46] S. Anders, A. Anders, I. G. Brown, B. Wei, K. Komvopoulos, J. W. Ager, and K. M. Yu, Surf. Coat. Technol. **68**, 388 (1994).

[47] D. Liu, G. Benstetter, E. Lodermeier, C. Xi, D. Jianning, L. Yanhong, Z. Jialiang, and M. Tengcai, Diam. Relat. Mater. **12**, 1594 (2003).

[48] M. Bonelli, A. C. Ferrari, A. Fioravanti, A. Li Bassi, A. Miotello, and P. M. Ossi, Eur. Phys. J. B **25**, 269 (2002).

[49] G. Zilibotti and M. C. Righi, Langmuir **27**, 6862 (2011).

[50] F. P. Bowden and J. E. Young, Proc. R. Soc. London A Mat. **208**, 444 (1951).

[51] J. Fontaine, P. I. Mech. Eng. J.-J. Eng. **222**, 1015 (2008).

[52] I. L. Singer, R. N. Bolster, J. Wegand, S. Fayeulle, and B. C. Stupp, Appl. Phys. Lett. **57**, 995 (1990).

[53] J. A. Greenwood and J. B. P. Williamson, Proc. R. Soc. London A Mat. **295**, 300 (1966).

[54] G. Zilibotti, M. C. Righi, and M. Ferrario, Phys. Rev. B **79**, 075420 (2009).

[55] O. Manelli, S. Corni, and M. C. Righi, J. Phys. Chem. C **114**, 7045 (2010).

[56] Y. Qi, E. Konca, and A. T. Alpas, Surf. Sci. **600**, 2955 (2006).